PROTEIN—SOLVENT INTERACTIONS

Pt2

about the book . . .

This practical resource covers the **latest advances** in the interactions of proteins with their solvent environment and provides fundamental physical information useful for the application of proteins in biotechnology and industrial processes. It discusses **in detail** structural, dynamic, and thermodynamic aspects of protein hydration as well as proteins in aqueous and organic solvents as they relate to protein function, stability, and folding.

Presenting integrated analyses of the most recent results, ***Protein–Solvent Interactions*** examines the construction of proteins and the protein devices that underlie protein function and stability, furnishing a new paradigm for protein research . . . reviews x-ray crystallographic results on the patterns of solvent structure in and around proteins . . . studies protein hydration, glass transitions, and the plasticizing action of water, leading to a unifying description of protein dynamics . . . highlights results from dielectric relaxation, Rayleigh scattering of Mossbauer radiation, positron annihilation lifetime spectroscopy, hydrogen isotope exchange, and flash photolysis techniques . . . outlines Brownian dynamics, Kramers's theory, and the effects of solvent viscosity on protein dynamics . . . defines the thermodynamic nonideality of proteins in water-cosolvent mixtures in terms of excluded volume and preferential interactions, supplying a **new appreciation** of binding phenomena . . . offers an inventory of solvent-induced effects on protein stability, association, and folding **and** shows how to obtain the missing thermodynamic data . . . introduces a **new approach** to protein separation problems . . . and much more.

With over **1000** bibliographic citations and some **500** equations, tables, and figures, ***Protein–Solvent Interactions*** is an incomparable reference for biochemists, biophysicists, physical chemists, biotechnologists, microbiologists, molecular biologists, pharmacologists, food technologists, and graduate-level students in these disciplines.

about the editor . . .

ROGER B. GREGORY is an Associate Professor in the Department of Chemistry at Kent State University, Ohio. The author of over 50 professional papers, book chapters, and abstracts that reflect his research interests in the areas of enzyme kinetics, protein conformational dynamics, protein hydration, and positron annihilation lifetime spectroscopy, he is a member of the American Chemical Society, the Biophysical Society, the American Society for Biochemistry and Molecular Biology, and the Biochemical Society. Dr. Gregory received the B.Sc. (1976) and Ph.D. (1980) degrees in biochemistry from the University of Sheffield, England.

Printed in the United States of America ISBN: 0–8247–9239–4

marcel dekker, inc./new york • basel • hong kong

64. Morgan, H., and R. Pethig, *J. Chem. Soc., Faraday Trans. 1, 82*: 143–156 (1986).
65. Bone, S., J. Eden, P. R. C. Gascoyne, and R. Pethig, *J. Chem. Soc. Faraday Trans. 1, 77*: 1729–1732 (1981).
66. Behi, J., S. Bone, H. Morgan, and R. Pethig, *Int. J. Quantum Chem., Quant. Biol. Symp. 9*: 367–374 (1982).
67. Lawton, B. A., Z. H. Lu, R. Pethig, and Y. Wei, *J. Mol. Liquids 42*: 83–98 (1989).
68. Bone, S., *Biochim. Biophys. Acta 1078*: 336–338 (1991).
69. Careri, G., M. Geraci, A. Giansanti, and J. A. Rupley, *Proc. Natl. Acad. Sci. USA 82*: 5342–5346 (1985).
70. Careri, G., A. Giansanti, and J. A. Rupley, *Proc. Natl. Acad. Sci. USA 83*: 6810–6814 (1986).
71. Rupley, J. A., L. Siemankowski, G. Careri, and F. Bruni, *Proc. Natl. Acad. Sci. USA 85*: 9022–9025 (1988).
72. Nagle, J. F., and M. Mille, *J. Chem. Phys. 74*: 1367–1372 (1981).
73. Edsall, J. T., and H. A. McKenzie, *Adv. Biophys. 16*: 53–183 (1983).

5

Protein Dynamics: Hydration, Temperature, and Solvent Viscosity Effects as Revealed by Rayleigh Scattering of Mossbauer Radiation

VITALII I. GOLDANSKII AND
YURII F. KRUPYANSKII
Russian Academy of Sciences, Moscow, Russia

I. INTRODUCTION

In all contemporary models of enzyme action, the functional activity of enzymes is directly connected with the dynamic properties of proteins [1–6]. The investigation of protein dynamics is also of interest in its own right since it is well known that different and seemingly incompatible properties of proteins are often revealed by different experimental techniques. Thus, the available data from one group of experimental techniques makes one think of the protein as a solid body [7–9]. On the other hand, the data from another group of experimental methods depicts the protein as a strongly fluctuating structure [4,10,11].

Therefore, protein dynamics is currently studied by employing such powerful physical methods as nuclear magnetic resonance [12,13], neutron scattering [14], computer simulation of protein dynamics [15,16], x-ray dynamical analysis

(XRDA) [17,18], and Mossbauer absorption spectroscopy (MAS) [19–21], along with conventional research methods such as the deuterium exchange technique [11,22] and luminescence labeling [23]. It was qualitatively shown by these conventional methods that hydration degree and solvent composition strongly influence protein dynamics. It is to be noted that unlike the other experimental methods just mentioned, x-ray analysis, neutron scattering, and MAS belong to a group of methods that allow protein dynamics to be quantitatively described using the mathematics of Van Hove correlation functions [24].

In this chapter, data will be reviewed relating to the influence of hydration, temperature, and solvent composition on protein dynamics by means of yet another "correlation" technique, the Rayleigh scattering of Mossbauer radiation (RSMR).

II. BACKGROUND OF RSMR TECHNIQUE, BASIC EXPRESSIONS, AND APPROXIMATIONS

There are several surveys dealing with RSMR in which experimental and theoretical fundamentals of the method are considered in some detail [25–27].

In this chapter, we concentrate on some specific features of the application of RSMR to the study of protein–solvent systems (see also [28,29]).

Shown in Fig. 1 is a schematic of the RSMR experimental arrangement. Mossbauer radiation emitted by a ^{57}Co source mounted on a vibrator experiences Rayleigh scattering by electrons of a biopolymer B. The radiation scattered at the angle 2θ is measured by the detector D. In order to measure the elastic scattering fraction, an additional resonance adsorber is employed, which together with the

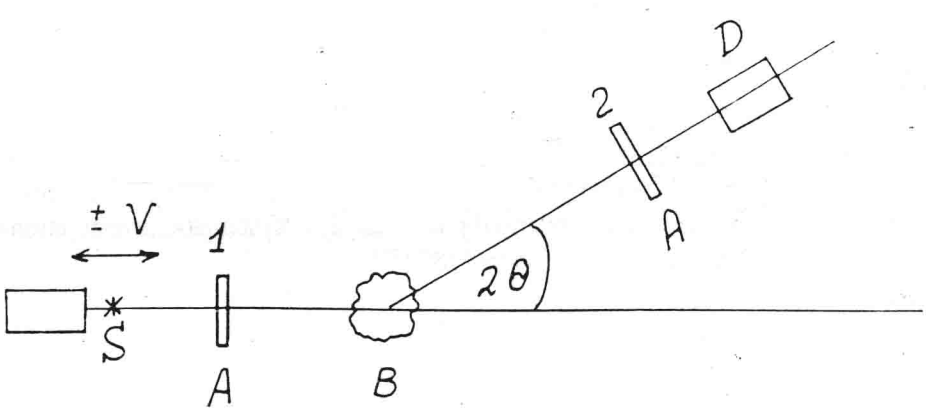

FIGURE 1 RSMR experimental setup. S is a Mossbauer source, B is a protein or other biopolymer under investigation, D is a detector, and A is a resonant absorber, which can alternatively be placed in positions 1 and 2 measure intensities $I(0)$ and $I(2\theta)$, respectively.

detector makes up the so-called Mossbauer detector. By means of the resonance absorber, first the intensity of the incident beam, $I(0)$, is measured and then the intensity of scattered radiation, $I(2\theta)$.

The elastic fraction is determined by

$$f = \frac{I_\infty(2\theta) - I_0(2\theta)}{I_\infty(0) - I_0(0)} \tag{1}$$

where I_0 and I are measured under the resonance condition (i.e., with the source velocity $V = 0$) and far away from resonance ($V = \infty$), respectively.

In measurements of the RSMR spectral lineshape, $\eta(\nu) = [I(\nu = \infty) - I(\nu)]/I(\nu = \infty)$, the resonance absorber is to be placed only in position 2. The Mossbauer source–detector combination accomplishes the high-energy resolution of the method ($\sim 10^{-9}$ eV), which exceeds by several orders of magnitude the resolution provided by the most advanced neutron spectrometers (up to $\sim 10^{-6}$ eV), let alone that offered by XRDA (~ 1 eV). It is precisely due to this fact that comparatively slow motion with correlation times from 10^{-6} to 10^{-9} s can be detected from broadening of energy spectrum lines and motions with correlation times $\tau_c < 10^{-9}$ s from the decrease of elastic scattering fraction.

The essential advantage of this method over MAS is its versatility, for the scatterer (the biopolymer under study) need not have Mossbauer nuclei. The scope of amenable biological objects thus can be substantially widened. In addition, the possibility of changing the scattering angle (or momentum transfer) in the course of an experiment and, as a consequence, the possibility of choosing relatively small scattering angles make it possible to obtain information on motions with much larger amplitudes than with MAS.

In its first application, RSMR was employed to distinguish between elastic and inelastic Rayleigh scattering intensity for polycrystalline and single-crystal [25] scatterers.

Further application of the RSMR technique to investigation of dynamical properties of inorganic single crystals, organic and polymeric glasses, and supercooled liquids has placed RSMR among the most effective methods for studying the dynamics of atoms in a condensed phase [25–27]. Systematic investigation of biopolymers by RSMR was begun in 1980 [30].

Results on the study of protein dynamics were obtained for a relatively long period by use of the so-called incoherent version of RSMR (see [28,29] and references therein), that is, the version in which soft collimation conditions were utilized. Usually, it is necessary to fulfill two conditions for the correct use of the incoherent approximation: (a) wide divergence of the beam and (b) remoteness of the scattering angle from the main Bragg maximum [26]. For intensity reasons and to provide, in the first approach, the quantitative study of RSMR spectra, only the first condition was realized in these works. The incoherent approach may not be strictly correct in this case. The low angular resolution of the experiment, how-

ever, produced strong averaging of the interference pattern. RSMR data analyzed with the incoherent approach may therefore certainly reveal some physical features of protein dynamics.

Recently, protein dynamics were also studied by RSMR in an angular-dependent fashion with good angular resolution ("coherent" version) in order to analyze the influence of coherent effects [31,32]. Since the counting rate in these experiments is rather poor, only a few results have been obtained up to now.

Below are considered the main approximations necessary to apply formulas to data obtained from RSMR experiments.

The dependence of the intensity J of scattered γ-quanta versus momentum $\mathbf{Q}$ ($\mathbf{Q} = (4\pi \sin\theta)/\lambda$, λ = wavelength) and energy $\hbar\omega$ transfer is connected with the double differential cross section $d^2\sigma/d\Omega\, d\omega$ and in a first-order approximation is given by [33]

$$J(\mathbf{Q}, \omega) = \frac{d^2\sigma}{d\Omega\, d\omega} = \bar{\bar{r}}_0^2 p_0^2 \sum_{m,n} S_{mn}(\mathbf{Q}, \omega) \tag{2}$$

where

$$\bar{\bar{r}}_0 = \frac{e^2}{mc^2}; \qquad p_0^2 = \frac{1}{2}(1 + \cos^2 2\theta)$$

The scattering function $S_{mn}(\mathbf{Q}, \omega)$ contains all the structure and dynamic information on the scattering system and in the case of RSMR is represented by

$$S_{mn}(\mathbf{Q}, \omega) = \frac{1}{2\pi} \int dt \exp\left(\frac{-i\omega t - \Gamma|t|}{2\hbar}\right) I_{mn}(\mathbf{Q}, t) \tag{3}$$

where

$$I_{mn}(\mathbf{Q}, t) = \sum_{m,n} \phi_m \phi_n \langle \exp[-i\mathbf{Q}R_m(t)] \exp[i\mathbf{Q}R_n(0)] \rangle \tag{4}$$

is the so-called intermediate correlation function, and $\phi_i(\mathbf{Q})$ is the atomic form factor of the ith atom.

The case of hydrated proteins will be mainly discussed in this section (the crystalline case [32], which is much simpler to treat, will be touched on only briefly).

Let us now discuss only proteins and then come to the more complicated situation of water–protein systems (hydrated proteins or proteins in a solvent).

The dynamics of proteins can be considered in the following simple approach. This model introduces a division of atoms of the protein globule into two parts. The first group (fraction) of atoms (A) move collectively within segments with a mean square displacement (msd) $\langle x^2 \rangle_s$. Motional correlations between different moving segments are neglected. Another fraction of atoms (B) moves indi-

vidually with $\langle x^2\rangle_i$, and motional correlations between different atoms and between atoms and segments are also neglected. In this case, the inelastic scattering intensity can be expressed as

$$J_{\text{inel}}(\mathbf{Q}) = \sum_S S_s(\mathbf{Q})\,[1 - \exp(-\mathbf{Q}^2\langle x^2\rangle_s)] + \sum_i \phi_i^2(\mathbf{Q})\,[1 - \exp(-\mathbf{Q}^2\langle x^2\rangle_i)] \tag{5}$$

If one considers, for simplicity, that $\langle x^2\rangle_i = \langle x^2\rangle_s = \langle x^2\rangle$, it leads to the following expression:

$$\begin{aligned} J_{\text{inel}}(\mathbf{Q}) &= [1 - \exp(-\mathbf{Q}^2\langle x^2\rangle)]\left[\sum_S S_s(\mathbf{Q}) + \sum_i \phi_i^2(\mathbf{Q})\right] \\ &= [1 - \exp(-\mathbf{Q}^2\langle x^2\rangle)][AS_{\text{SEG}}(\mathbf{Q}) + BF_i^2(\mathbf{Q})] \end{aligned} \tag{6}$$

where $A + B = 1$, $S_{\text{SEG}}(\mathbf{Q})$ represents the interference pattern from the collectively moving segment and $\mathbf{F}_i^2(\mathbf{Q}) = \sum_i \phi_i^2(\mathbf{Q})$, the sum here extending over all atoms moving individually.

Then elastic and total scattering intensity, by analogy with [32], can be written as follows:

$$\begin{aligned} J_p(\mathbf{Q},\infty) &= S_0^{\,p}(\mathbf{Q})\exp(-\mathbf{Q}^2\langle x^2\rangle_p) \\ J_p(\mathbf{Q},0) &= S_0^{\,p}(\mathbf{Q})\exp(-\mathbf{Q}^2\langle x^2\rangle_p) \\ &\quad + [AS_{\text{SEG}}^2(\mathbf{Q}) + BF_{ip}^2(\mathbf{Q})][1 - \exp(-\mathbf{Q}^2\langle x^2\rangle_p)] \end{aligned} \tag{7}$$

Here $S_0^{\,p}(\mathbf{Q})$ represents the interference pattern from the whole protein sample. One then obtains, for the elastic fraction,

$$f_p(\mathbf{Q}) = \frac{S_0^{\,p}(\mathbf{Q})\exp(-\mathbf{Q}^2\langle x^2\rangle_p)}{S_0^{\,p}(\mathbf{Q})\exp(-\mathbf{Q}\langle x^2\rangle_p) + [AS_{\text{SEG}}{}^{P}(\mathbf{Q}) + BF_{ip}^2(\mathbf{Q})][1 - \exp(-\mathbf{Q}^2\langle x^2\rangle_p)] + J_c} \tag{8}$$

where J_c is the Compton scattering intensity. It is quite instructive to consider the limiting cases. If the motional correlations extend over the whole sample $B = 0$, $A = 1$, $S_{\text{SEG}}{}^p = S_0^{\,p}(\mathbf{Q})$, and

$$f_p(\mathbf{Q}) = \frac{S_0^{\,p}(\mathbf{Q})\exp(-\mathbf{Q}^2\langle x^2\rangle_p)}{S_0^{\,p}(\mathbf{Q}) + J_c} \tag{9}$$

If all atoms within the globule move independently from each other, then $A = 0$, $B = 1$. This leads to

$$f_p(\mathbf{Q}) = \frac{S_0^{\,p}(\mathbf{Q})\exp(-\mathbf{Q}^2\langle x^2\rangle_p)}{S_0^{\,p}(\mathbf{Q})\exp(-\mathbf{Q}^2\langle x^2\rangle_p) + F_{ip}^2(\mathbf{Q})[1 - \exp(-\mathbf{Q}^2\langle x^2\rangle_p)] + J_c} \tag{10}$$

Neglecting all interference terms for the elastic and inelastic scattering, one can come to the incoherent approximation:

$$S_0(\mathbf{Q}) = \sum_i \phi_i^2; \quad S_{\text{SEG}}(\mathbf{Q}) = \sum_i \phi_i^2$$

and

$$f_p(\mathbf{Q}) = \frac{\sum_i \phi_i^2(\mathbf{Q}) \exp(-\mathbf{Q}^2\langle x^2\rangle_p)}{\sum_i \phi_i^2(\mathbf{Q}) + J_c} = \frac{F_{ip}^2(\mathbf{Q}) \exp(-\mathbf{Q}^2\langle x^2\rangle)}{F_{ip}^2(\mathbf{Q}) + J_c} \tag{11}$$

Now consider the protein–water system. We shall use the following physical assumptions for analysis of the data: (a) For hydrated proteins (as distinct from crystalline samples), the complete absence of correlation in the location of one globule relative to another is suggested; that is, the scattering function of hydrated protein $S_p(\mathbf{Q})$ contains interference terms only from one protein globule. (For crystalline samples, the scattering function $S_p(\mathbf{Q})$ contains interference terms from all protein atoms in the crystal since the intensity is the sum from all unit cells [32].) (b) Correlation in locations of different water molecules is essential; therefore, $S_w(\mathbf{Q})$ contains interference terms from oxygen atoms of different water molecules. (c) Correlation in locations of different protein and water molecules relative to one another will be neglected (i.e., the corresponding interference terms will be considered as small).

With these assumptions, the intensity of the γ-quanta Rayleigh scattered by the protein–water system is the sum of intensities

$$J_\Sigma(\mathbf{Q}) = J_p(\mathbf{Q}) + J_w(\mathbf{Q}) \tag{12}$$

Since the hydration water is in general far more mobile than the atoms of the protein, the description demands the introduction of different msd for interprotein water, as compared with protein.

The elastic fraction for the water–protein system is equal to [26,29]

$$f_\Sigma = \frac{J_\Sigma^{\text{el}}(\mathbf{Q})}{J_\Sigma(\mathbf{Q}) + J_c} = C_p f_p + C_w f_w \tag{13}$$

In the case of the incoherent approximation, this leads to

$$f_\Sigma(\mathbf{Q}) = \frac{F_{ip}^2(\mathbf{Q}) \exp(-\mathbf{Q}^2\langle x^2\rangle_p) + F_i^2{}_w(Q) \exp(-\mathbf{Q}^2\langle x^2\rangle_w)}{F_{ip}^2(\mathbf{Q}) + F_i^2{}_w(Q) + J_c} \tag{14}$$

For a truly coherent treatment, the division of f_Σ into separate contributions is not possible due to pair correlations between protein and water. Fortunately, these correlations play a minor role at sufficiently large scattering angles and at the wide divergence of the beam employed (see assumption c). The following attempt can be made to include, at least in part, coherent effects. If Eq. (9) is as-

sumed valid and pair correlations between protein and water are neglected, one can arrive, after averaging over scattering angle, at the expression [34]

$$\begin{aligned}\langle f\Sigma(\mathbf{Q})\rangle_{\Delta Q} &= \langle C_p\rangle_{\Delta Q} f_p + \langle C_w\rangle_{\Delta Q} f_w \\ &= \frac{f_p + h\langle C_1\rangle_{\Delta Q} f_w}{1 + h\langle C_1\rangle_{\Delta Q} + \langle C_2\rangle_{\Delta Q}} \\ &\quad + \frac{\langle i_p(\mathbf{Q})\rangle_{\Delta Q} f_p + \langle i_w{}^b(\mathbf{Q})\rangle_{\Delta Q} h C_1 f_w}{1 + h\langle C_1\rangle + \langle C_2\rangle_{\Delta Q}}\end{aligned} \tag{15}$$

where h is the hydration degree, ΔQ is the divergence of the beam

$$i(\mathbf{Q}) = S(\mathbf{Q}) - 1$$

$$C_1 = \frac{\phi_w{}^2 + J_c{}^w}{\phi_p{}^2 + J_c{}^P}$$

and

$$C_2 = \frac{\phi_p{}^2 i_p(\mathbf{Q}) + h\phi_w{}^2 i_w{}^b(\mathbf{Q})}{\phi_p{}^2 + J_c{}^p}$$

For the protein component, the scattering functions $S_0{}^p(\mathbf{Q})$ and $i_p(\mathbf{Q})$ can be either calculated from crystallographic coordinates or taken from experiments on dry protein. Of course, then we have to assume that no changes occur in the interatomic distances when drying or crystallizing protein. For the water component, the situation is much more difficult. It is well known that the structural and dynamical properties of interprotein (bound) water are drastically different from those for free water [35]. Strongly bound water assumes a lacy structure on the protein surface [36]. Therefore, it is natural to suggest that at one extreme the scattering function for interprotein waters, $S_w{}^b(\mathbf{Q})$, and consequently the function $i_w{}^b(\mathbf{Q})$, coincides with the scattering function for protein

$$i_w(\mathbf{Q}) = i_w{}^b(\mathbf{Q}) = i_p(\mathbf{Q}) \tag{16}$$

At the other extreme, the scattering function for interprotein water coincides with the scattering function for free (bulk) water

$$i_w(\mathbf{Q}) = i_w{}^f(\mathbf{Q}) \tag{17}$$

The numerical relationship given in Eq. (15) strongly depends on the value of the average scattering angle 2θ and the shape of the angular resolution function B, or divergence of the beam ΔQ. For the RSMR setup used in [28,29], $2\theta = 11.9°$, the angular resolution function is described by a Gaussian with a width $\sigma = 2.4°$ and the average values of $\langle i_i(\mathbf{Q})\rangle_{\Delta Q}$ are the following:

$$\begin{aligned}&\langle i_p(\mathbf{Q})\rangle_{\Delta Q} \simeq 0.1 \quad \text{for met-Mb and HSA} \\ &\langle i_w(\mathbf{Q})\rangle_{\Delta Q} \simeq 0.2 \quad \text{for free water}\end{aligned} \tag{18}$$

According to the convolution hypothesis [38], an intermediate correlation function (see Eq. (4)), in which cooperative motions of different atoms are taken into account, may be represented by

$$I(\mathbf{Q}, t) = S(\mathbf{Q})I_s(\mathbf{Q}, t) = [1 + i(\mathbf{Q})]I_s(\mathbf{Q}, t) \tag{19}$$

The intermediate self-correlation function $I_s(\mathbf{Q}, t)$ contains information about essentially more simple individual motions of atoms and atomic groups.

It is easy to show that with this approximation, a relationship similar to (15) is valid for the spectral function that retains the nontrivial terms of η (ν):

$$g_\Sigma(\mathbf{Q}, \omega) = C_p g_p(\mathbf{Q}, \omega) + C_w g_w(\mathbf{Q}, \omega) \tag{20}$$

where

$$C_p = \frac{1 + i_p(\mathbf{Q})}{1 + hC_1 + C_2}; \qquad C_w = hC_1 \frac{1 + i_w(\mathbf{Q})}{1 + hC_1 + C_2}$$

and

$$g_{p,w}(\mathbf{Q}, \omega) = \frac{1}{2\pi} \int dt \exp\left(\frac{-i\omega t - \Gamma|t|}{2\hbar}\right) I_s^{p,w}(\mathbf{Q}, t)$$

Certainly, all assumptions made in deriving Eq. (15) are included in Eq. (20).

It is quite evident that for incoherent evaluation an expression similar to (20) is valid [29].

The use of a Gaussian approximation [37,38] for the self-correlation function $I_s(\mathbf{Q},t)$ gives the possibility to come finally to the following expression for the lineshape:

$$g_{p,w}(\mathbf{Q}, \omega) = \frac{1}{2\pi} \int dt \exp\left(-i\omega t - \frac{\Gamma|t|}{2\hbar}\right) \exp\left(-\frac{1}{2}\mathbf{Q}^2\langle[x(t) - x(0)]^2\rangle\right) \tag{21}$$

Here $\langle\ \rangle$ denotes an ensemble average and $x(t)$ is the coordinate of the atom at time t.

III. HYDRATION DEPENDENCIES OF THE ELASTIC RSMR FRACTIONS AND RSMR SPECTRA

If assumption (16) holds for interprotein water, expression (15) can be rewritten numerically as

$$\langle f_\Sigma(\mathbf{Q})\rangle_{\Delta Q} = \frac{f_p + 1.21hf_w}{1 + 1.21h} \tag{22}$$

that is, when scattering functions for interprotein water and protein coincide, the expression for the elastic fraction is identical to the expression obtained with the

incoherent approximation. If, on the contrary, interprotein water behaves like free water (Eq. (17)), the elastic fraction will have the numerical form

$$\langle f_\Sigma(\mathbf{Q})\rangle_{\Delta Q} = \frac{f_p + 0.9hf_w}{1 + 0.9h} \tag{23}$$

In this case, the expression for the elastic fraction is slightly different from that obtained in the incoherent approximation. Within this suggestion on interprotein water properties, even wide divergence of the beam does not average the coherent phenomena.

Figure 2 shows a typical hydration curve of the elastic fraction f_Σ, for human serum albumin (HSA), obtained at room temperature [40,41].

A straightforward analysis of relationships (22) and (23) leads to the conclusion that there is no additivity of dynamical properties in the HSA–water system in the entire range of hydration studied. Indeed, if we use $f_\Sigma(h \to 0)$ for f_p, $f_p = f_\Sigma(0) = 0.8$, and assume $f_w = 0$, as for free water, then the calculated curve for f_Σ, shown as a dotted line in Fig. 2 (see Eq. (23)), exhibits large deviations from the experimental data. For all hydration degrees studied, adding more water not only does not give the contribution to the elastic RSMR (quite in accord with $f_w = 0$), but further loosens the protein, increasing its mobility and reducing the value

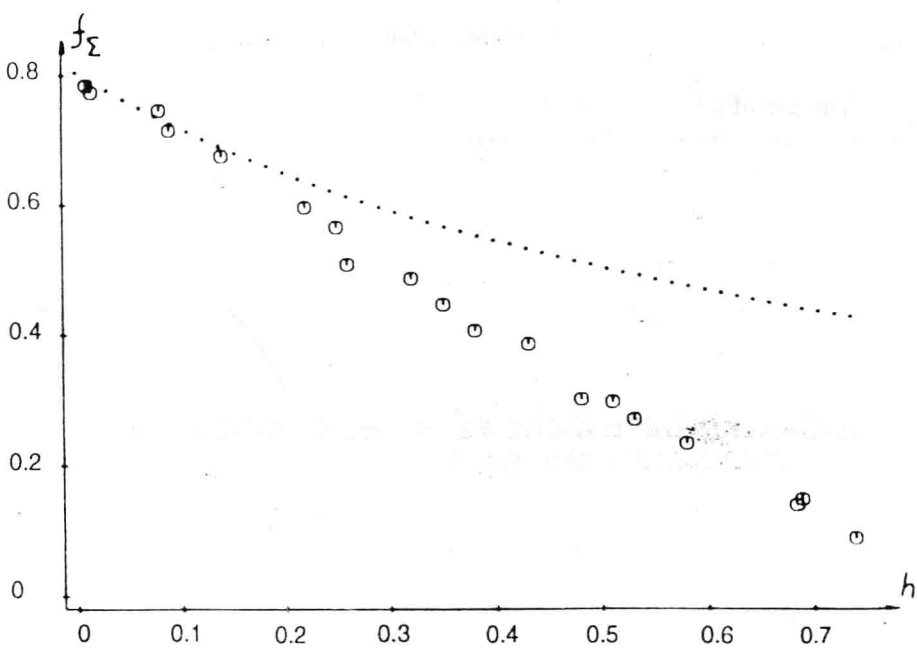

FIGURE 2 Hydration dependence of the elastic scattering fraction for an HSA sample. Dotted line is calculation in terms of Eq. (23) assuming no interaction between dry protein and free water.

of f_p. Thus, at all hydration levels investigated, $0.05 < h < 0.75$, dynamical properties of HSA are influenced by its water content. This conclusion is in no way linked to the assumptions that $f_w = 0$ or the validity of Eq. (17). Let us consider a more realistic picture of bound-water behavior. It is well known from the literature [42] that small amounts of water, up to 10% of dry protein weight, are strongly bound to the protein. According to NMR and ESR data, relaxation properties exhibited by bound water at large h, about 0.4 to 0.5, are typical of common liquids with viscosity greater than that of free water but lower than that of glycerol. Hence, at the other extreme, structural (see Eq. (16)) and dynamical properties of bound water coincide in the entire range of hydration degrees with those of the protein (see also Eq. (22)).

Shown in Fig. 3 is a family of dependencies calculated, in terms of Eqs. (22) and (23), of the elastic scattering fraction for the protein alone, ϕf_p, among which is contained the real curve representing the actual variation of the protein dynamics. The symbol ϕ denotes a calculated value rather than a measured one. The lower boundary of the cross-hatched range of ϕf_p values corresponds to the assumption that dynamical and structural properties of interprotein water are not different from those of protein for all tested values of h, and the upper one to the assumption that the water behaves as free water. The real curve of the hydration dependence of protein dynamical properties, $\phi f_p^*(h)$, shown in Fig. 3 as a heavy line, was calculated under the following assumptions: at small hydration degrees, $h \leq 0.1$, the dynamical properties of bound water are no different from those of the protein; then, at greater h, they are like those of viscous liquids, $f_w \rightarrow 0.05$ (the

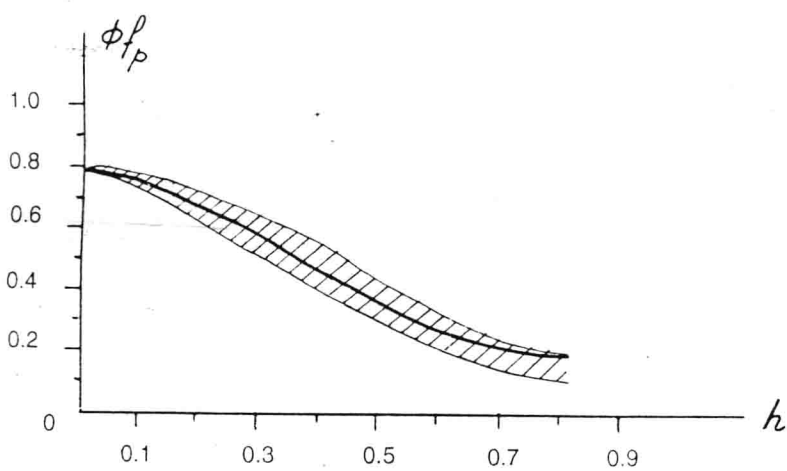

FIGURE 3 Calculated elastic fraction ϕf_p as a function of the hydration degree on the basis of Eqs. (22) and (23). Different assumptions were made concerning the behavior of the interprotein water. Details are given in the text.

magnitude of the elastic fraction for glycerol at $T = 295$ K [43]); approaching the dynamical properties of free water, $f_w = 0$, with $h \geq 0.6$ to 0.7. As seen from Fig. 3, even under these more realistic assumptions about the behavior of bound water, there still will be no additivity of dynamical characteristics in the HSA–water system in the entire hydration range studied.

The absence of additivity of the dynamical properties of water–protein systems is displayed in the dependence of the real curve, $\phi f_p^*(h)$, on h. Figure 4 shows the area under the total spectrum, S_Σ, from a metmyoglobin sample (met-Mb, $M = 17{,}800$) as a function of the hydration degree, h (in this series of measurements, spectra were taken only for a narrow velocity range, -2.3 to 2.3 mm/s). As in the case of HSA (see Fig. 2), the dotted line is calculated with Eq. (23). Shown in Fig. 5 is a family of curves $\phi S_p(h)$ calculated by using Eqs. (22) and (23) along with the realistic curve $\phi S_p^*(h)$. As one can see from Fig. 5, there is no additivity of the dynamical properties in the met-Mb–water system up to the value of $h = 0.6$ g/g. Addition of more water above this value can be seen to have very little effect on the dynamical properties of met-Mb.

Elsewhere, we have also studied hydration dependencies for trypsin ($M = 23{,}319$) [44] lysozyme ($M = 14{,}000$) [40], DNA ($M = 1$ to 3×10^6 amu) [45] and chromatophores ($M = 10^7$ amu) [46]. Hydration of all these biopolymers has been found to result in a reduction of the real elastic fraction, $\phi f_p^*(h)$, and, therefore, to

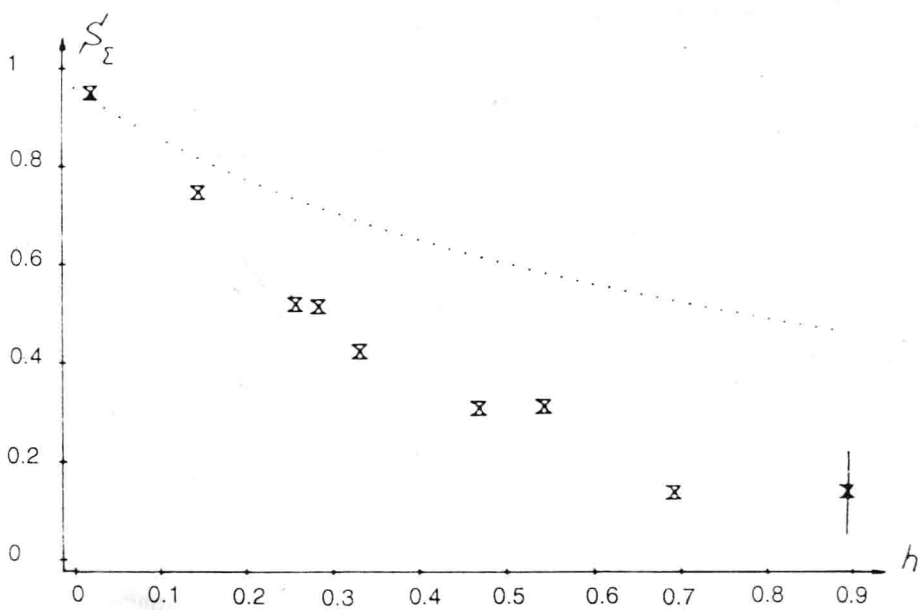

FIGURE 4 Hydration dependence of the area under the total spectrum, S_Σ, for met-Mb. Dots represent calculation under the same assumptions as in Fig. 2.

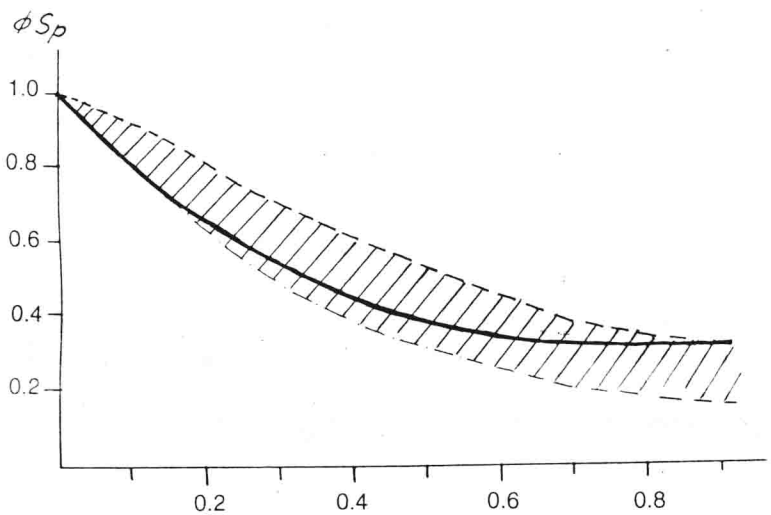

FIGURE 5 Calculated area, $\phi S_p(h)$, for met-Mb. See Fig. 3 for explanation. Heavy line is the realistic curve $\phi S_p^*(h)$.

an increase in values of $\langle x^2 \rangle(h)$ for hydration degrees $0.05 < h < 0.5$ (one exception is lysozyme, where the addition of water beyond $h = 0.35$ has no effect on the dynamical properties of the protein).

Presented in Fig. 6 are RSMR energy spectra for met-Mb (for three degrees of hydration) [47], obtained over a large range of measurement velocities, $V = \pm 20$ mm/s. At large hydration degrees, $h \geq 0.6$, neither spectrum can be described by a single Lorentzian (even admitting broadening). To describe the total spectrum, a second quasi-elastic line has to be included (a "wide" component). The presented spectra are a sum of a narrow line with a width equal to the width at $h = 0$ and a "wide" line.

IV. SOLVENT COMPOSITION AND VISCOSITY DEPENDENCIES OF THE ELASTIC RSMR FRACTIONS

We have also studied the influence of viscosity, or, more precisely, solvent composition, on the dynamics of proteins and chromatophores [48,49]. A number of papers have appeared recently describing direct experimental observations of the influence of solvent viscosity on the rate of biochemical reactions [50,51] and the theoretical treatment of these data [52,53]. As a rule, it is suggested [50–53] that the solvent viscosity directly influences protein dynamics, which, in its turn, determines protein reactivity. Direct experimental evidence, however, for the influence of viscosity on protein dynamics has yet to be obtained. Therefore, we have attempted to observe directly this influence, and these attempts will be described

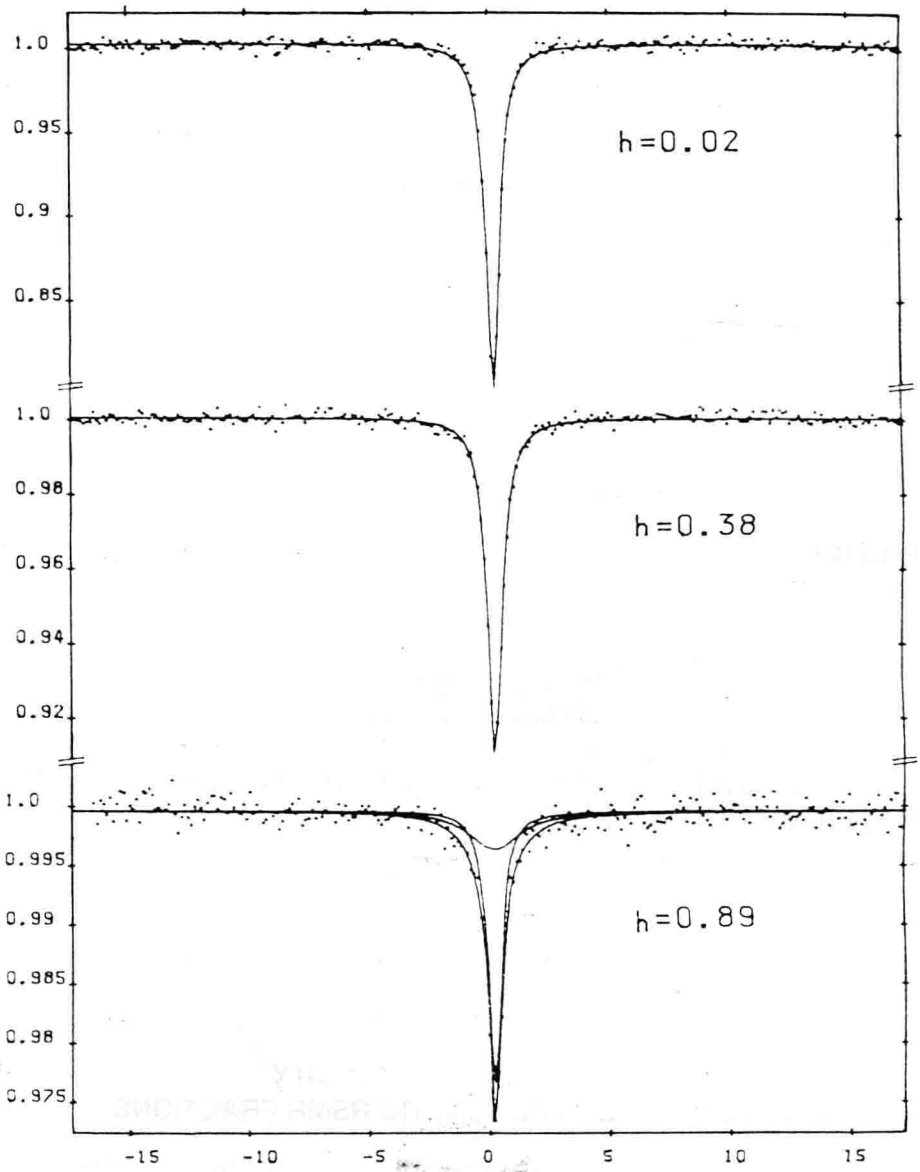

FIGURE 6 Energy spectra of met-Mb samples with different degrees of hydration.

in this section. Temperature dependencies of the elastic fraction for three samples shown in Fig. 7 were studied: I, 37% water solution of HSA; II, 37% water solution of HSA with the addition of 7.5% (by weight) of glutaric dialdehyde (GD); and III, water–glycerol solution of HSA with relative content of protein equal to 34%, water 22%, and glycerol 44%.

The addition of GD in water solution transforms sample I from the liquid to the solid state (sample II) and, consequently, leads to a very large increase in macroviscosity. Sample III (water–glycerol–protein solution) preserves fluidity and, hence, has lower visible viscosity than sample II. Nevertheless, the visible influence of water–glycerol solvent on protein dynamics is much stronger than that of GD (see Fig. 7). This fact suggests that it is the microviscosity in the vicinity of the protein surface that plays the crucial role in influencing protein dynamics.

These effects were evaluated within the framework of the incoherent approximation (see Eqs. (11) and (14)). As will be seen, more advanced treatment is impossible now because of the lack of knowledge about structural properties of water–glycerol mixtures. Anyway, as was mentioned in Sec. II, the incoherent treatment can give us a satisfactory qualitative picture.

Additional experimental temperature dependencies of the elastic fraction for water—$f_w(T)$, glycerol—$f_G(T)$, and water–glycerol solution were studied to deduce dynamical information on the protein. These curves are represented in Fig. 8.

For samples I and II, Eqs. (14) and (15) can be rewritten numerically [49] as

$$\phi f_p(T) = 3.09 f_\Sigma(T) - 2.09 f_w(T) \tag{24}$$

There exist some variants to take into account contributions of the solvent for sample III (protein in water–glycerol solution): (a) To take into account the contribu-

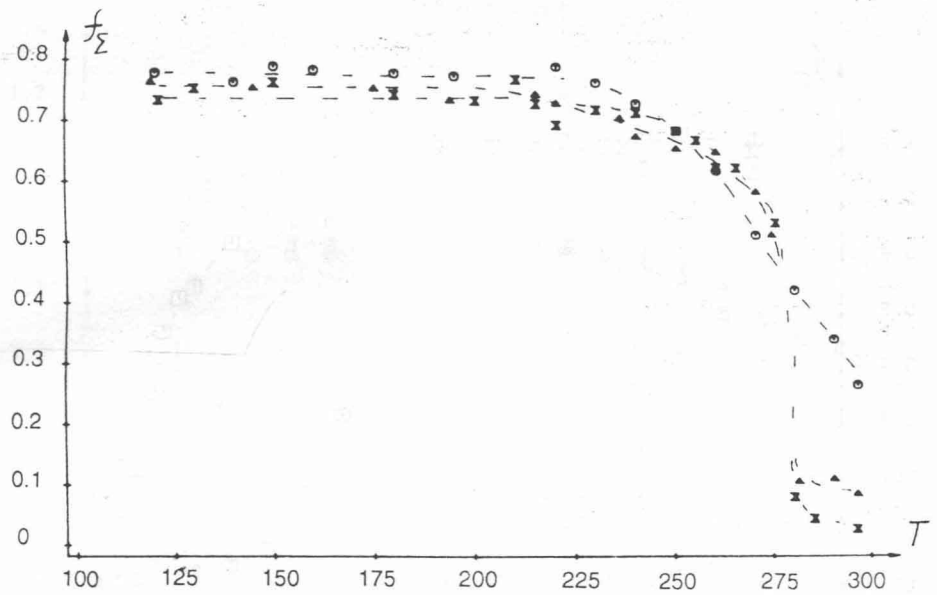

FIGURE 7 Experimental temperature dependencies of elastic fraction for 37% water solution of HSA (⊠), the same solution with the addition of 7.5% of GD (▲), and a water–glycerol solution of HSA (⊙).